



UNIVERSITÀ
DI TORINO

Characterization of Hadronic Showers in the Belle II Electromagnetic Calorimeter

Emanuele Zanusso

Dipartimento di Fisica
Università degli Studi di Torino

January 14, 2026

Outline

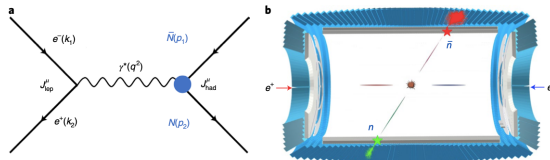


- 1. Anti-neutrons in physics experiments**
- 2. Preliminary study via signal Monte Carlo sample**
- 3. Study of Monte Carlo cocktail**
- 4. Outlook**

Anti-neutron in HEP experiments

The \bar{n} plays a key role in several physics measurements, such as:

- The neutron e.m. form factor studies in $e^+ + e^- \rightarrow n + \bar{n}$ process



- Some decay channels studied at B-factories which involve \bar{n}
 1. The hyperons decay channel:
$$\bar{\Lambda}^0 \rightarrow \pi^0 + \bar{n}, \quad \bar{\Sigma}^- \rightarrow \pi^- + \bar{n}, \quad \bar{\Lambda}_c \rightarrow K_s^0 + \pi^0 + \bar{n}$$
- Discrimination between other neutral particles (γ) and \bar{n}

Anti-neutrons in astrophysics

The \bar{n} also plays a key role in several astrophysics measurements, such as:

- Studying \bar{n} - anti-hyperon potential to improve the understanding of the equation of state of the neutron stars
- Investigating dark matter through anti-deuterons (\bar{D}) in cosmic rays, produced by dark matter annihilation or decay

$A_{d.m.} + B_{d.m.} \rightarrow \text{hadrons } (n, \bar{n}, p, \bar{p} \text{ etc...})$

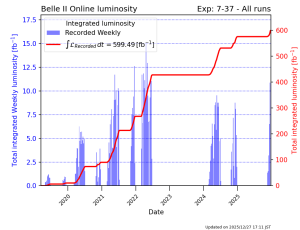
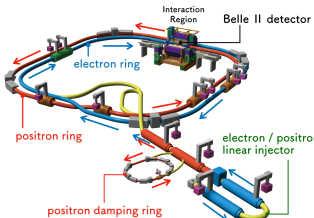
$X_{d.m.} \rightarrow \text{hadrons } (n, \bar{n}, p, \bar{p} \text{ etc...})$

\bar{D} is mainly produced through a coalescence mechanism $\bar{n} + \bar{p} \rightarrow \bar{D}$,
where \bar{p} and \bar{n} are nearby in the phase-space

The Belle II experiment

SuperKEKB is an asymmetric $e^+ e^-$ collider (Tsukuba, Japan)

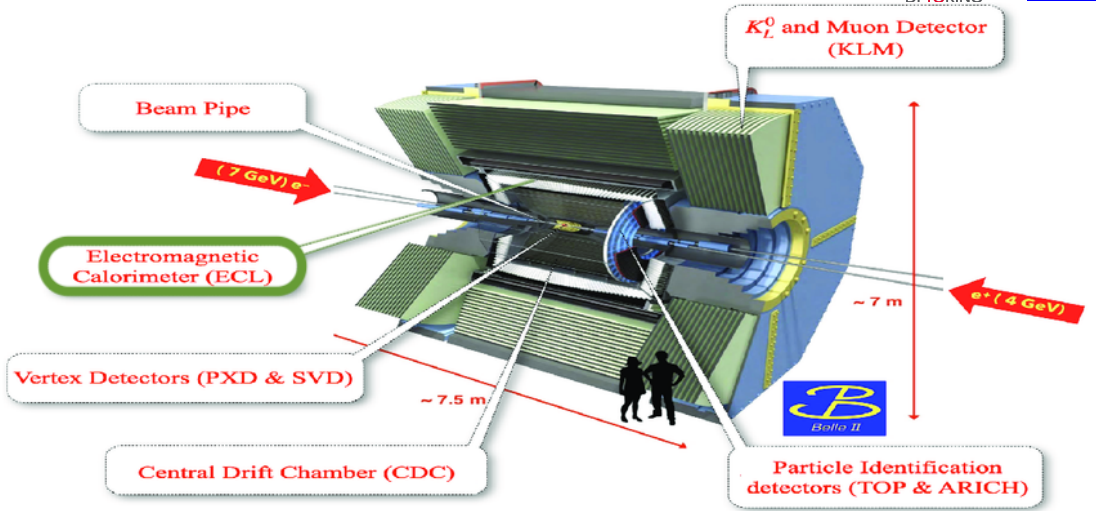
- 7 GeV electron beam (HER)
- 4 GeV positron beam (LER)
- Peak Luminosity $\sim 5.1 \times 10^{34} cm^{-2}s^{-1}$
- Design Luminosity $\sim 8 \times 10^{35} cm^{-2}s^{-1}$
→ x40 the Belle's one



It operates mainly around $\Upsilon(4S)$ resonance (~ 10.58 GeV):

- This resonance decays almost exclusively into entangled couples of $B\bar{B} \rightarrow B$ -factory
- Several goals: flavour physics, BSM physics, heavy hadrons spectroscopy etc...

The Belle II experiment

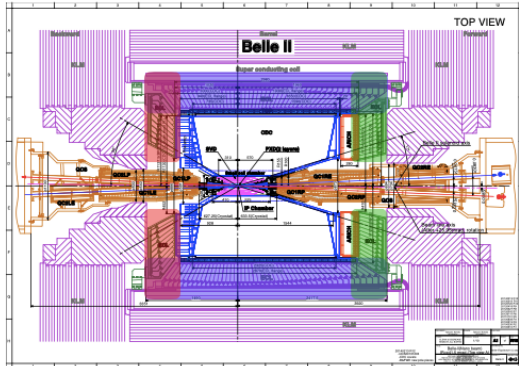


The Electromagnetic Calorimeter

The ECL plays a central role in this thesis

- Array of **CsI(Tl)** crystals (8376 $6 \times 6 \times 30 \text{ cm}^3$ crystals in total)
- It covers barrel and end-cap regions ($12^\circ \leq \theta \leq 155^\circ$)
- Energy resolution of 4% @100 MeV and 1.6% @8 GeV

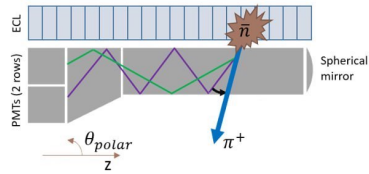
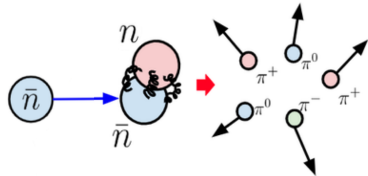
Barrel
FWD endcap
BWD endcap



Anti-neutron interactions in physics

The \bar{n} interacts primarily via strong nuclear force, producing hadronic showers
It can annihilate with nucleons in the ECL, producing light mesons (mainly pions)

- π^0 decays into $\gamma\gamma$, producing electromagnetic showers that are fully contained in the ECL
- π^\pm undergo hadronic interactions, which are not fully contained in the ECL → both the forward (KLM) and backward (TOP) directions are involved



The MANTRA project (PRIN2022)

Measuring Anti-Neutron: Tagging and Reconstruction Algorithm



- A general method to measure the $E_{\bar{n}}$ up to 10 GeV, by combining information from:
 1. A detector with high time resolution (TOP)
 2. An electromagnetic calorimeter (**ECL**)
 3. A muon system (KLM)
- These features are common in modern general-purpose collider experiments such as **Belle II** and BESIII, which do not have a dedicated calorimeter
- For MANTRA project, only signals from ECL and TOP are taken into account. In this thesis only ECL signals are studied

Are \bar{n} hadronic showers correctly simulated in the Belle II software?

The MANTRA project

LA LEVO????? Anti-neutrons cannot be reconstructed by sub-detectors.

The measurement of the energy is a two-step process:

1. \bar{n} identification via its induced ECL clusters (study of the shower shape)
2. Combine the signals from TOP and ECL to reconstruct the \bar{n} energy, in cases of backscattering or pre-showering
 - If π^0 ($\sim 5\%$): energy is all contained in the calorimeter, the shower is fully reconstructed
 - If π^\pm ($\sim 95\%$): their products may escape the crystals
→ the goal is to complement the calorimeter information with that from the adjacent detectors

Preliminary concept

Several channels can be selected to look at \bar{n} annihilations, such as:

- $e^+ + e^- \rightarrow p + \bar{n} + \pi^- + (\gamma_{ISR})$ (Mine)
- $\bar{\Lambda}_c \rightarrow K_s^0 + \pi^0 + \bar{n}$
- $\Lambda(\rightarrow p + \pi^-) + \bar{\Lambda}(\rightarrow \bar{n} + \pi^0)$

Several variables can be used to validate the showers shape for \bar{n} identification, \bar{n} identification via its induced ECL clusters (study of the shower shape) such as:

- **Zernike Moments**, which describe cluster shape (backup)

$$\bullet \text{ **Lateral momentum** defined as: } C_{LM} = \frac{\sum_{i=2}^n \omega_i E_i r_i^2}{\omega_0 E_0 r_0^2 + \omega_1 E_1 r_1^2 + \sum_{i=2}^n \omega_i E_i r_i^2}$$

$$\bullet \text{ **Second moment** defined as: } C_{SM} = \frac{\sum_{i=0}^n \omega_i E_i r_i^2}{\sum_{i=0}^n \omega_i E_i}$$

Analysis outline

1. Study of the selected signal channel $e^+ + e^- \rightarrow p + \bar{n} + \pi^- + (\gamma_{ISR})$
 - (a) Recoil identification from the system $p + \pi^-$ (with and without ISR)
 - (b) Study of the kinematic recoil variables (momentum, angles, energy, etc...)
 - (c) Study of the effect of 1C kinematic fit over the recoil mass
 - (d) Study of ECL shower shape variables
2. Study of MC cocktail sample:
 - (a) Recoil identification from the system $p + \pi^-$ (with and without ISR)
 - (b) Study of the kinematic recoil variables (momentum, angles, energy, etc...)
3. Study of real data sample:
 - (a) Recoil identification from the system $p + \pi^-$ (with and without ISR)
 - (b) Constraint with 1C kinematic fit over the recoil mass
 - (c) Examine Data/MC agreement in ECL cluster shapes from \bar{n} channel

Analysis outline (1)

- The analyzed channel is:

$$e^+ + e^- \rightarrow p + \bar{n} + \pi^- + (\gamma_{ISR})$$

The reconstructed particles are (cuts and selections in the next slide):

- (a) $p + \pi^- + (\gamma_{ISR})$ which compose the recoil system
- (b) Neutral clusters associated to \bar{n} candidates list used to compare its variables with those of the recoil

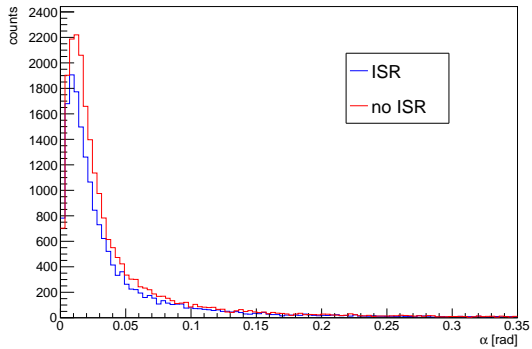
rowNo	decay tree	decay final state	iDcyTr	nEtr	nCEtr
1	$vpho \rightarrow \pi^- \bar{n}p$	$\pi^- \bar{n}p$	0	35291	35291
2	$e^+ e^- \rightarrow vpho \gamma^I \gamma^J, vpho \rightarrow \pi^- \bar{n}p$	$\pi^- \bar{n}p \gamma^I \gamma^J$	2	22971	58262
3	$e^+ e^- \rightarrow vpho \gamma^I, vpho \rightarrow \pi^- \bar{n}p$	$\pi^- \bar{n}p \gamma^I$	1	18735	76997
4	$vpho \rightarrow \pi^- \bar{n}p \gamma^F$	$\pi^- \bar{n}p \gamma^F$	3	10005	87002
5	$e^+ e^- \rightarrow vpho \gamma^I \gamma^J, vpho \rightarrow \pi^- \bar{n}p \gamma^P$	$\pi^- \bar{n}p \gamma^I \gamma^J \gamma^P$	6	5274	92276
6	$e^+ e^- \rightarrow vpho \gamma^I, vpho \rightarrow \pi^- \bar{n}p \gamma^P$	$\pi^- \bar{n}p \gamma^I \gamma^P$	4	4621	96897
7	$vpho \rightarrow \pi^- \bar{n}p \gamma^F \gamma^P$	$\pi^- \bar{n}p \gamma^F \gamma^P$	7	1503	98400
8	$e^+ e^- \rightarrow vpho \gamma^I \gamma^J, vpho \rightarrow \pi^- \bar{n}p \gamma^P \gamma^F$	$\pi^- \bar{n}p \gamma^I \gamma^J \gamma^P \gamma^F$	8	700	99100
9	$e^+ e^- \rightarrow vpho \gamma^I, vpho \rightarrow \pi^- \bar{n}p \gamma^F \gamma^P$	$\pi^- \bar{n}p \gamma^I \gamma^F \gamma^P$	5	597	99697
10	$vpho \rightarrow \pi^- \bar{n}p \gamma^F \gamma^P \gamma^F$	$\pi^- \bar{n}p \gamma^F \gamma^P \gamma^F$	9	167	99864
11	$e^+ e^- \rightarrow vpho \gamma^I, vpho \rightarrow \pi^- \bar{n}p \gamma^F \gamma^F \gamma^F$	$\pi^- \bar{n}p \gamma^I \gamma^F \gamma^F \gamma^F$	12	63	99927
12	$e^+ e^- \rightarrow vpho \gamma^I \gamma^J, vpho \rightarrow \pi^- \bar{n}p \gamma^F \gamma^F \gamma^P$	$\pi^- \bar{n}p \gamma^I \gamma^J \gamma^F \gamma^F \gamma^P$	10	61	99988
13	$e^+ e^- \rightarrow vpho \gamma^I, vpho \rightarrow \pi^- \bar{n}p \gamma^F \gamma^F \gamma^F \gamma^P$	$\pi^- \bar{n}p \gamma^I \gamma^F \gamma^F \gamma^F \gamma^P$	11	4	99992
14	$e^+ e^- \rightarrow vpho \gamma^I \gamma^J, vpho \rightarrow \pi^- \bar{n}p \gamma^F \gamma^F \gamma^F \gamma^F$	$\pi^- \bar{n}p \gamma^I \gamma^J \gamma^F \gamma^F \gamma^F \gamma^F$	15	4	99996
15	$vpho \rightarrow \pi^- \bar{n}p \gamma^F \gamma^F \gamma^F \gamma^P$	$\pi^- \bar{n}p \gamma^F \gamma^F \gamma^F \gamma^P$	14	2	99998
16	$vpho \rightarrow \pi^- \bar{n}p \gamma^F \gamma^F \gamma^F \gamma^F \gamma^P$	$\pi^- \bar{n}p \gamma^F \gamma^F \gamma^F \gamma^F \gamma^P$	13	1	99999
17	$e^+ e^- \rightarrow vpho \gamma^I \gamma^J, vpho \rightarrow \pi^- \bar{n}p \gamma^F \gamma^F \gamma^F \gamma^F \gamma^P$	$\pi^- \bar{n}p \gamma^I \gamma^J \gamma^F \gamma^F \gamma^F \gamma^F \gamma^P$	16	1	100000

- 100k events.** The reconstruction efficiency is:

$$\epsilon = \frac{n^{\circ} \text{ of reconstructed candidates}}{n^{\circ} \text{ of generated events}} \sim 22\%(18\%)$$

Applied selections and cuts

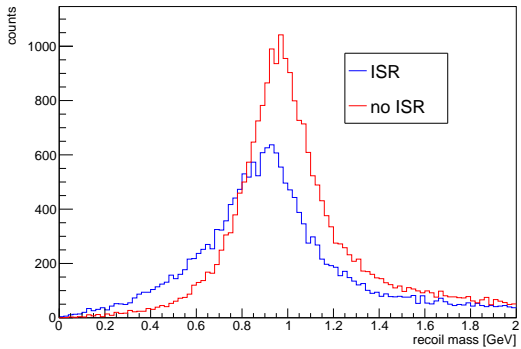
- (a) **proton**: standard PID selection, with tracks required to originate from the IP
- (b) **pion**: standard PID selection
- (c) **anti-neutron**: neutral clusters from ECL
- (d) $0 \text{ GeV} < \text{recoil mass} < 2 \text{ GeV}$
- (e) $\alpha < 0.35 \text{ rad} (\sim 20 \text{ deg})$



Where α is the angle between the recoil vector direction and the closest \bar{n} cluster

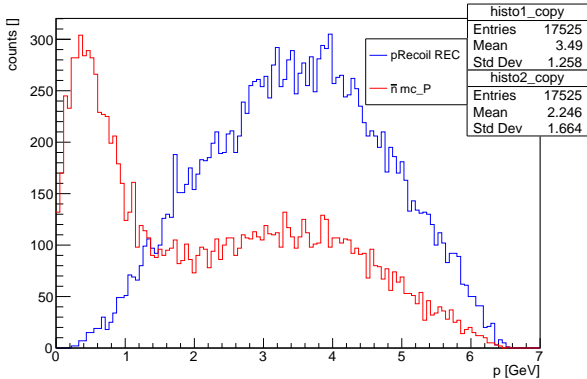
The recoil mass

- The recoil mass is well reconstructed in both ISR (p, π^-, γ_{ISR}) and no ISR (p, π^-) cases
 - Variables associated with the \bar{n} candidate clusters can be compared with the reconstructed recoil variables (p, θ)
- Since there is more than one γ_{ISR} per event, the  distribution shows a higher number of entries in the left tail



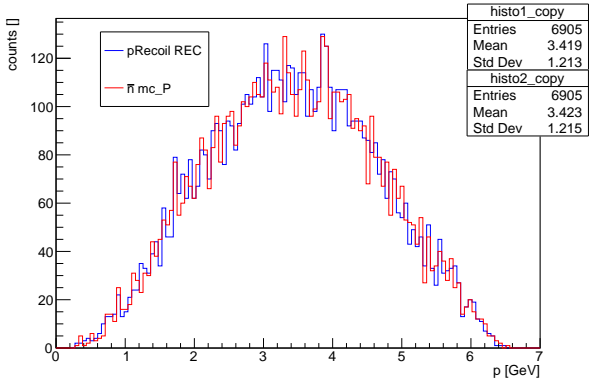
The recoil and the \bar{n} momentum

- The reconstructed \bar{n} candidate list shows a discrepancy with the recoil momentum \rightarrow several γ are mis-identified as \bar{n} in reconstruction
- MC selection $\bar{n}_{mcPDG} = -2112$ is applied in order to directly compare the recoil kinematic variables with the \bar{n} from MC truth (next slide)



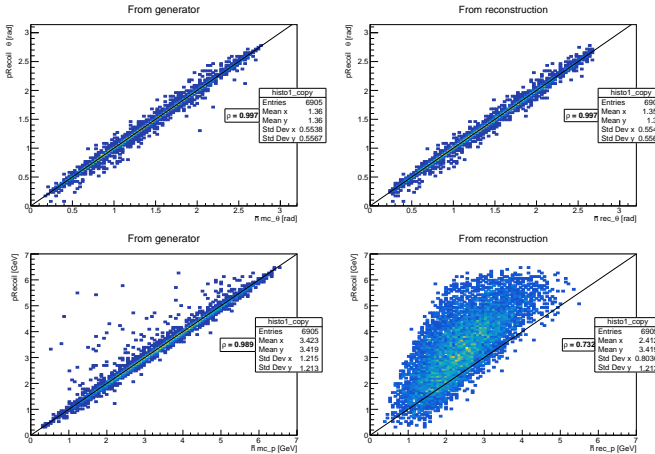
The recoil and the \bar{n} momentum

- Among the 17525 reconstructed candidates, 6905 correspond to real \bar{n} .
 - (a) 100000 generated events
 - (b) 17525 reconstructed events ($\sim 18\%$)
 - (c) 6905 real \bar{n} in candidates list ($\sim 7\%$)
- For a ($LUMI$) real data, ($TOTevents$) are expected



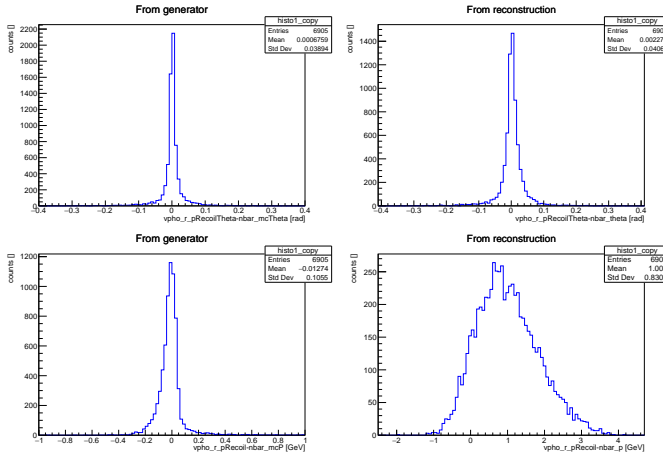
\bar{n} vs recoil vector correlation

- Good correlation is observed at the generator level in both the momentum and θ distributions
- The reconstructed \bar{n} momentum in the ECL is not a reliable variable, since no high correlation is observed (annihilation and energy loss)



\bar{n} vs recoil vector residuals

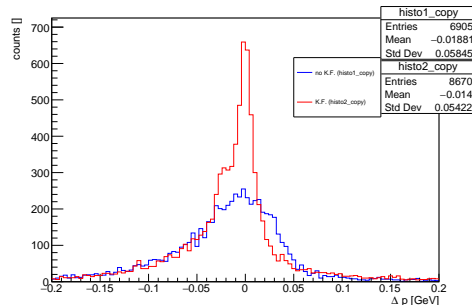
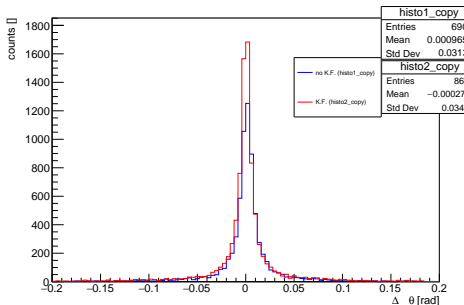
- Good correlation is observed at the generator level in both the momentum and θ distributions
- The reconstructed \bar{n} momentum in the ECL is not a reliable variable, since no high correlation is observed (annihilation and energy loss)



Kinematic Fit over the recoil mass

A 1C kinematic fit can possibly be used to add a constraint and improve the agreement in p and θ

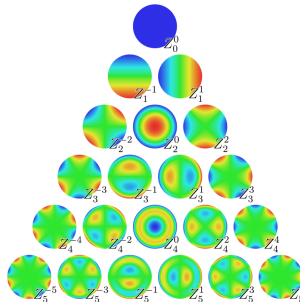
- Highest amount of reconstructed candidates ($\sim 24\%$) and of real \bar{n} ($\sim 9\%$)
- No significant differences can be seen in θ_{recoil} vs MC $\theta_{\bar{n}}$
- An improvement can be observed in p_{recoil} vs MC $p_{\bar{n}}$



\bar{n} ECL cluster variables

Shower shapes variables can be studied to distinguish \bar{n} from other neutral particles:

- **E, E1E9 and E9E21**
($E_{min} = 20$ GeV)
- **ZernikeMoment51**: $|Z_{51}|$



10	11	12	13	14
25	2	3	4	15
24	9	1	5	16
23	8	7	6	17
22	21	20	19	18

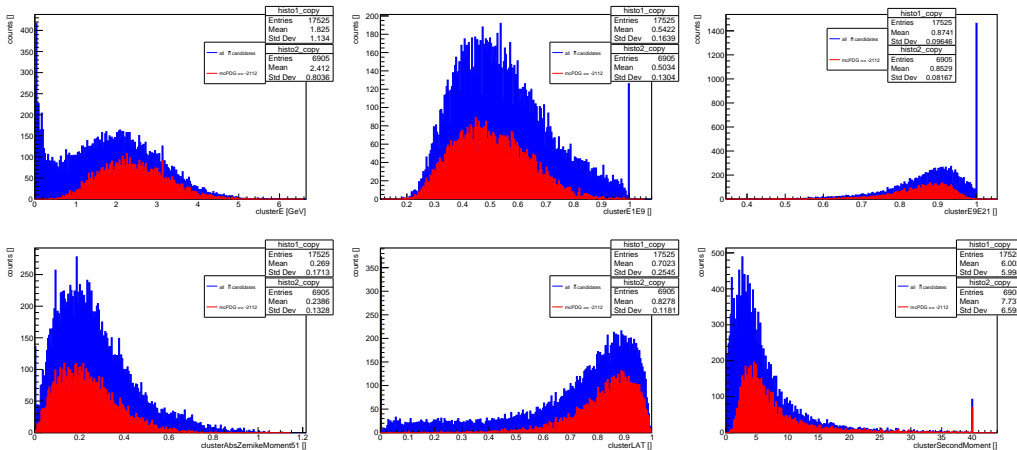
- **Lateral momentum**: lateral energy distribution, defined as:

$$S = \frac{\sum_{i=2}^n \omega_i E_i r_i^2}{\omega_0 E_0 r_0^2 + \omega_1 E_1 r_1^2 + \sum_{i=2}^n \omega_i E_i r_i^2}$$

\bar{n} ECL cluster variables



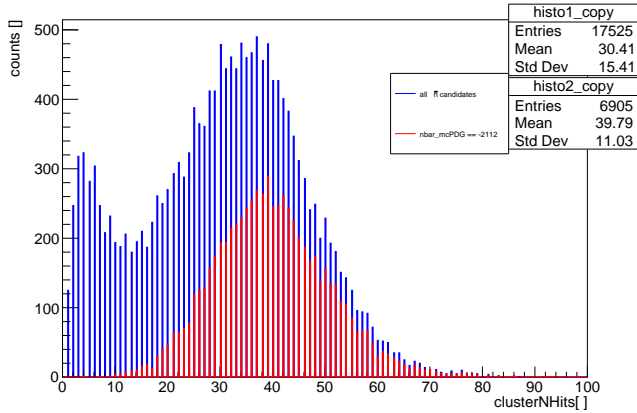
UNIVERSITÀ
DI TORINO



\bar{n} ECL cluster variables

- \bar{n} clusters mainly involve 15 or more crystals
- Several photons are mis-identified as \bar{n} during reconstruction (backup) → further selection can be studied such as:

$\bar{n}_{mcPDG} \neq 22$
 &&
 $\bar{n}_{clusterNHits} > 15$



Summary (1)

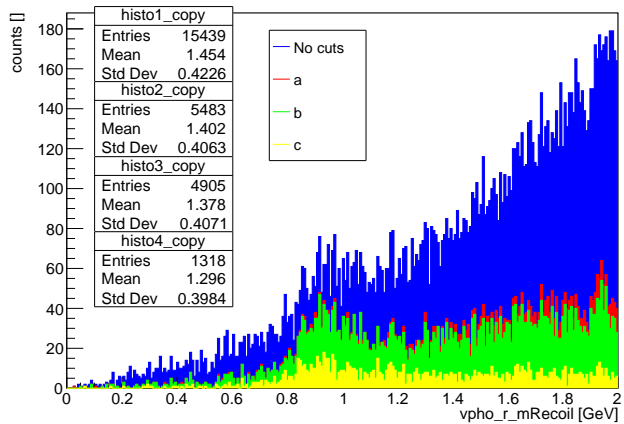
- Channel $e^+ + e^- + \gamma_{ISR} \rightarrow X \rightarrow p + \bar{n} + \pi^-$ has been studied
- The recoil three body system ($p + \pi^- + \gamma_{ISR}$) is correctly reconstructed from the secondary background, ISR/FSR photons
- The \bar{n} kinematic is properly described by the three body system p, π^-, γ recoil vector
- Reconstructed \bar{n} variables are mainly affected by mis-identified photons, which can be partially cleaned by cluster size cuts (*clusterNHits*)
- 1C kinematic fit can be possibly adopted during MC/Data comparison, in order to improve the recoil on the recoil momentum

Analysis outline (2)

- Study of cocktail from MC16rd_proc16 using the following MC sample:
 - (a) $q\bar{q}$ cocktail powered by Pythia
 - (b) Number of Events: $341 M$
 - (c) Luminosity: $215 fb^{-1}$
- To obtain a first attempt, only the p and π^- are used to build the recoil vector (ISR neglected for the moment)
- 2345 jobs have been submitted to the grid, with the following online cuts:
 1. $p_mcPDG == 2212$ and $pi_mcPDG == -211$ and $0 \text{ GeV} < m\text{Recoil} < 2 \text{ GeV}$
 2. The best candidate is selected with RankByLowest method on α (backup)
- Same strategy as before:
 - (a) Identify the signal peak near the \bar{n} mass ($\sim 0.939 \text{ GeV}$) adding offline cuts
 - (b) Study the previous variables (recoil and cluster) in a $m\text{Recoil}$ zoomed region
 - (c) (3) Compare it with data (Data/MC agreement)

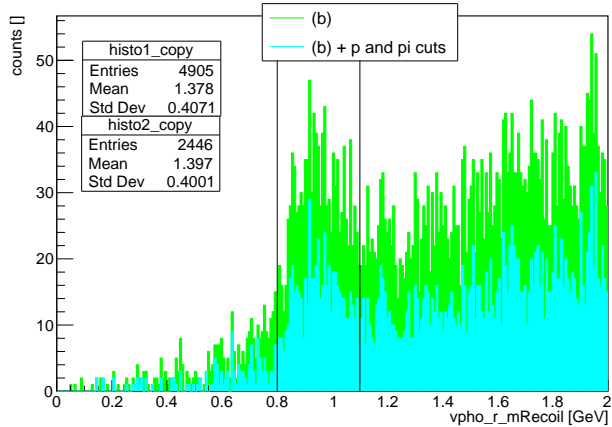
mRecoil distribution

- The following cuts are applied to enhance the signal:
 - $nRoeCharged == 0$ (no additional charged particles in the Rest Of Event)
 - $nRoeCharged == 0$ and $\alpha < 0.35$ (additional angular cut on the closest candidate)
 - $nRoeCharged == 0$ and $\alpha < 0.35$ and $nbar_mcPDG == -2112$ (MC truth selection)



mRecoil distribution

- “Real selections” can be applied as well, with (b), such as: [longo2025]
 $\text{protonID} > 0.9$ and $\text{pionID} > 0.1$ and $\text{dr} < 1$ and $\text{abs(dz)} < 3$ (from IP) ■■■
- To maximize purity, a recoil mass selection in the range (0.8-1.1) GeV can be applied to study the recoil variables
- This set of selections will be applied in the following sections



Variables

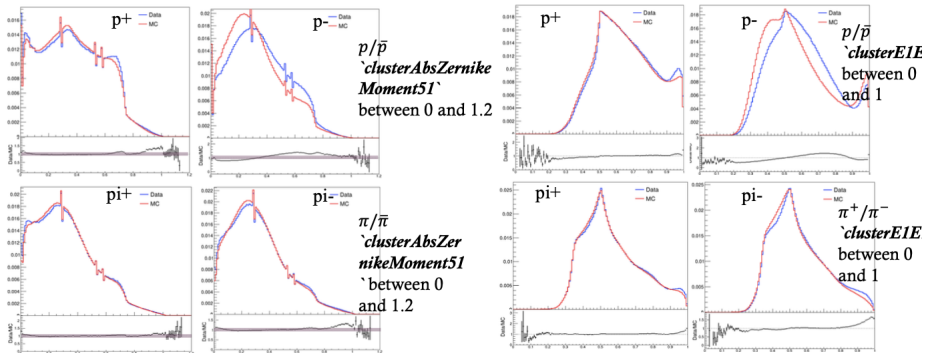


Summary (2)



Data/MC agreement \bar{n} case

Analysis of a $\Lambda \rightarrow p + \pi^-$ ($\bar{\Lambda} \rightarrow \bar{p} + \pi^+$) sample shows that [shanette2025]:



Poor Data/MC agreement in $\bar{p} \rightarrow$ will it be the same for \bar{n} ?

Outlook Until Graduation





UNIVERSITÀ
DI TORINO

Thank you for your attention

Emanuele Zanuso

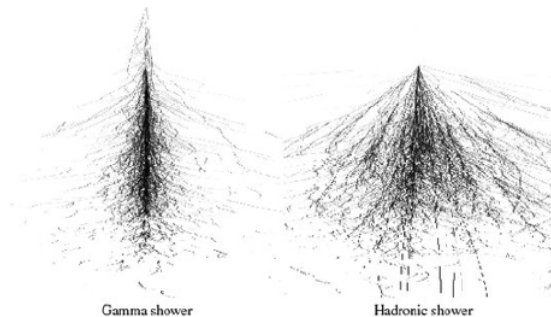
Dipartimento di Fisica
Università degli Studi di Torino

January 14, 2026

Electromagnetic and hadronic showers

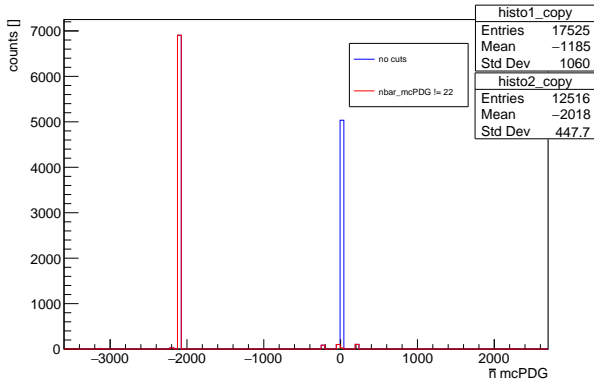
Different processes occur for e.m. (1) and hadronic (2) showers:

1. Bremsstrahlung and pair production process (e^+, e^-, γ) and $\pi^0 \rightarrow \gamma\gamma$
 2. Strong interactions of hadrons with the material ($p, n, pions, kaons...$)
- About the 95% of the hadronic shower is contained within a cylinder of radius λ_{had} (~ 44.12 cm in CsI(Tl))
 - About the 90% of the e.m. shower is contained within a cylinder of radius R_M (~ 3.6 cm in CsI(Tl))



\bar{n} mcPDG I

γ 's are mis-identified as \bar{n} in reconstruction:



UNIVERSITÀ
DI TORINO

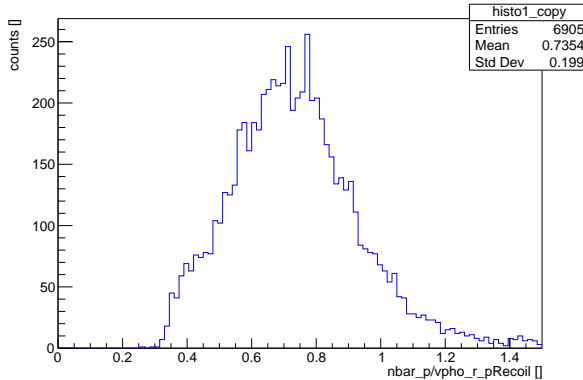


$p_{\bar{n}}/\text{pRecoil}$ |

\bar{n} is underrated in the most of cases (annihilation process + loss of energy)



UNIVERSITÀ
DI TORINO



References I

